PERGAMON

International Journal of Impact Engineering 24 (2000) 733–746

INTERNATIONAL JOURNAL OF IMPACT ENGINEERING

www.elsevier.com/locate/ijimpeng

Impact perforation resistance of laminated and assembled composite plates

Dahsin Liu[a,*], Basavaraju B. Raju[b], Xinglai Dang[a]

[a]*Department of Materials Science and Mechanics, Michigan State University, East Lansing, MI 48824, USA*
[b]*U.S. Army Tank-automotive Research, Development & Engineering Center (TARDEC), Warren, MI 48397, USA*

Received 20 March 1999; received in revised form 9 March 2000

Abstract

A previous study on impact response of composite laminates concluded that impact perforation was the most important damage stage in composite laminates subjected to impact loading since impact characteristics and degradation of mechanical properties of composite laminates reached critical levels once perforation took place. It was also found that thickness had a greater influence on impact perforation resistance than in-plane dimensions. However, as the composite laminates became very thick, the manufacturing cost for obtaining high-quality composite laminates could become unaffordable. In an effort to meet design requirements and to reduce manufacturing costs, assembled composite plates, which were organized by assembling multiple thin composite laminates together, were considered as alternatives to thick laminated composite plates. Various joining techniques including mechanical riveting, adhesive bonding, stitching and their combinations were used in assembling two- and four-laminate plates. Experimental results revealed that epoxy bonding outperformed other joining techniques. Although good bonding resulted in a higher impact bending stiffness and subsequently a higher perforation threshold, increasing the laminate thickness, or the number of laminates, was found to be more efficient in raising perforation threshold than improving the joining stiffness. As a major finding of the study, the assembled composite plates were found to have perforation thresholds similar to the laminated counterpart. Hence, the former could be used to replace the latter, at least, as far as perforation threshold was concerned.

Keywords: Laminated; Assembled; Composite plates; Penetration; Perforation

1. Introduction

Due to their high stiffness-to-weight and high strength-to-weight ratios, fiber-reinforced polymer–matrix composites are ideal materials for high-performance structures. They are usually used

* Corresponding author.

0734-743X/00/$ - see front matter
PII: S0734-743X(00)00021-X

in thin-laminate form. As composite technologies advance, more and more thick-section composites are used for heavy-duty structures. For example, the applications of thick composite laminates for submarine hull and armored vehicle bodies have proved to be feasible. The advancement from thin to thick laminates, however, is not trivial. It falls into a study categorized as scaling effect [1,2] and requires modifications and improvements in almost every aspect of composite technologies such as laminate theory, contact algorithm, manufacturing technique, etc. Since thick composite laminates behave quite differently from their thin counterparts, investigations on thick laminates have gained much attention [3].

Studies regarding the scaling effects on composite response to impact loading have been reported [4–6]. A similar study has been presented by the authors and their associates [7]. They have concluded in their study that perforation is the most important damage stage in composite laminates subjected to impact loading. The reason is that impact characteristics (such as peak force, contact duration and absorbed energy) and mechanical properties degradation (such as residual compressive maximum force and residual compressive absorbed energy) of composite laminates reach critical values when perforation takes place. They have also verified that thickness, as opposed to in-plane dimensions, has much greater influence on perforation resistance.

However, as composite laminates become thicker, the manufacturing cost for high-quality composite laminates may become unaffordable. For example, in order to achieve uniform curing and thus uniform properties through the thickness of thick composite laminates, expensive microwave curing process is required [8]. In an effort to meet the design requirements for high quality and to reduce the manufacturing costs, *assembled composite plates*, which are organized by assembling multiple thin composite laminates together, are considered as alternatives for thick *laminated composite plates* in this study.

In assembling thin composite laminates together, three fundamental joining techniques including adhesive bonding, mechanical fastening, and stitching are performed in this study. In addition, combined methods based on these three techniques are also explored. Both adhesive bonding and mechanical fastening have been well discussed in the literature. Being virtually the combination of adhesive bonding and mechanical fastening, stitching has also been found to be feasible for composite joining [9,10] and reinforcement [11]. Since it offers a relatively uniform load transfer in the structural components involved, its application to assembling thin laminates is also of interest in this study.

Accordingly, the objectives of this study are to (1) investigate the joining stiffness and perforation threshold of assembled composite plates based on various joining techniques, (2) identify an efficient way of assembling thin composite laminates for achieving a high perforation threshold, and (3) explore the feasibility of replacing the costly thick laminated composite plates by assembled composite plates.

2. Experimental methods

2.1. Thin composite laminates

Composite laminates made of glass fibers and an epoxy matrix were investigated in this study. The glass fibers were of E-glass type whereas the epoxy matrix was of 3M 1002 resin. The

composite laminates were of cross-ply type and had a stacking sequence of $[0/90/0/\ldots]_{13}$. The nominal fiber volume fraction of the composite laminates was about 53% and the averaged thickness was 3.2 mm. In this study, these composite laminates were assembled together to form two-laminate composite plates by using various joining techniques.

2.2. Impact testing

In order to characterize the perforation resistance of assembled composite plates, a DYNATUP GRC 8200 machine was used for impact testing. A schematic diagram of the impact testing machine was given in Fig. 1. According to the diagram, the impactor consisted of three components: a dropping crosshead, an impactor rod, and an impactor nose. The steel impactor rod had a diameter of 12.5 mm and was attached to the dropping crosshead. A force transducer having a capacity of 22.24 kN was mounted on the front end of the impactor rod and encapsulated by a hemispherical nose. The impactor was set at a dropping height of 0.91 m to give a constant impact velocity at 4.22 m/s for most tests. The total mass of the impactor, however, ranged from 10.35 to 17.74 kg (by adding various deadweights to the crosshead), resulting in impact energy from 92 to 158 J. For impact energy higher than 158 J, another similar impact testing machine with a pneumatic unit was used. The pneumatic unit was able to provide an additional force to increase the impact velocity up to 8 m/s.

In each impact test, a composite specimen with dimensions of 125 mm × 100 mm was placed between two steel plate holders, namely the top holder and the bottom holder as shown in Fig. 1.

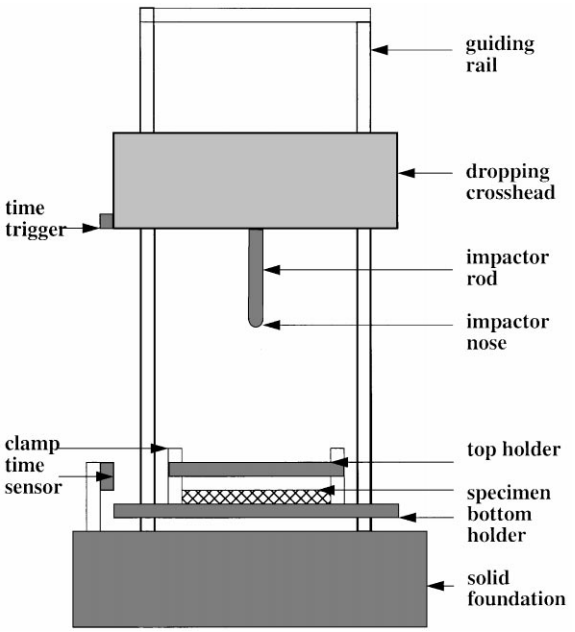

Fig. 1. Schematic diagram of impact testing machine.

Each holder had an opening of 100 mm × 75 mm in the center. The top holder was removable while the bottom one was attached to the frame of the impact testing machine which was fixed on a solid foundation. The specimen and the top steel holder were then C-clamped at four corners to the bottom steel holder. The composite specimen thus had a fixed boundary condition. In impact testing, the impactor contacted the center of composite specimens, resulting in so-called central impact.

In most impact tests, the crosshead was released from the preset height, and dropped freely according to the gravitational force. However, for impact tests with energy higher than 158 J, it was driven by both gravitational force and pneumatic force. As the impactor dropped and approached the composite specimen, its time trigger passed through a time sensor right before contact-impact occurred. The initial impact velocity was then calculated from the distance between two edges on the time trigger and the time interval they passes through the sensor. Once impact began, the contact forces at many consecutive instants were detected by the force transducer attached to the impactor. The force history was recorded in a computer. The corresponding velocity history of the impactor could then be calculated from integrating the force history (after being divided by the mass of the impactor) and using the initial impact velocity. Subsequently, the corresponding displacement history of the impactor could be calculated from integrating the velocity history.

Based on the force and displacement histories, the force–displacement relation and the energy history of the impactor could be established. Assuming the impactor was perfectly rigid and the energy loss on the contact–impact interface between the impactor and the specimen was negligible, the force–displacement relation of the impactor could be considered as the force–deflection curve of the composite specimen. And the kinetic energy of the impactor right before contact–impact took place, i.e. the *impact energy*, would be the energy transferred to the composite specimen. However, depending on the impact energy level and the type of specimen investigated, either a partial or the total amount of impact energy could be absorbed by the composite specimen in forms of damage, heat and others.

2.3. Joining techniques

In investigating assembled composite plates, the aforementioned 3.2-mm-thick glass/epoxy laminates were used as the building block. Many two-laminate composite plates were created. Each was formed by assembling two laminates together. Various joining techniques such as adhesive bonding, mechanical fastening, stitching joining, and their combinations were investigated.

In adhesive bonding, the bonding surfaces of composite laminates were roughened with emery papers to promote later mechanical interlocking. They were then cleaned with acetone before being coated with either a Scotch double-sided tape or a two-part room-temperature curing epoxy. The former was manufactured by 3M while the latter had a brand name EnviroTex Lite. These two types of adhesive bonding represented different degrees of bonding rigidity and strength. For convenience of discussion, the taped two-laminate composite plates were called 2T (2 for two-laminate and T for taped) while the epoxy-bonded two-laminate plate 2B (B for bonded).

In mechanical fastening, square riveting patterns with various densities, such as 2×2, 3×3, and 4×4 per each 50 mm × 50 mm area were created. Fig. 2 showed the details of the riveting patterns. In performing riveting, holes were prepared by a #30 drilling bit before 4×580 steel rivets (1/8″ in diameter and 1/4″ in grip) were pushed in by using a riveting gun. In addition, a circular riveting

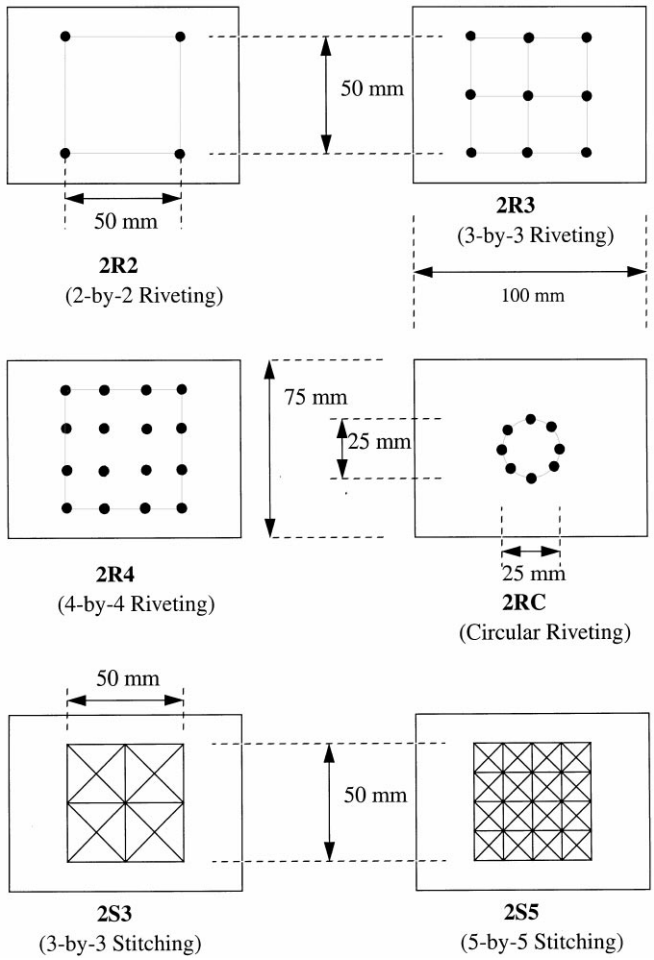

Fig. 2. Schematic diagrams of some riveting and stitching patterns.

pattern consisting of eight rivets uniformly located on the circumference of a 25-mm-diameter circle in the center of composite laminates was also employed in the study. These four riveting patterns were designated as 2R2, 2R3, 2R4 and 2RC. The first number of the designations, i.e. 2, again represented for two-laminate plates. The second letter R stood for riveting while the last number or letter gave riveting density or shape. That was, 2R2 was for 2×2, 2R3 was for 3×3, 2R4 was for 4×4, and 2RC was for circular riveting. The circular riveting 2RC was also included in Fig. 2.

Similar to riveting, several stitching patterns were also used in assembling two-laminate composite plates. A 28 gauge steel wire was used as the stitching thread with the stitching holes prepared by a drilling bit of 1/16″ in diameter. For each four holes forming a square unit, six stitching lines, two longitudinal, two horizontal and two diagonal as shown in Fig. 2 were performed on each side of the composite plates. The stitching joints were prepared by pulling the stitching thread through the stitching holes as tightly as possible by hand. Stitching densities

of 3×3, 5×5, and 9×9 per each 50 mm × 50 mm area were investigated. They were denoted as 2S3, 2S5, and 2S9, respectively, where 2 was for two-laminate plates, S was for stitching, and the last number represented for stitching densities. Fig. 2 also showed the stitching patterns of 2S3 and 2S5.

In addition to the individual joining techniques presented above, two-laminate composite plates were also assembled by using combined joining techniques. A 2BR3 plate was assembled by both epoxy bonding (B for bonded) and a 3×3 riveting pattern (R for riveting) and a 2BS3 assembled plate combined both epoxy bonding and a 3×3 stitching pattern (S for stitching). The investigations of these combined joining techniques were part of the study in search of higher joining rigidity and strength.

3. Results and discussions

3.1. Force–deflection curves

Before studying assembled composite plates, the composite laminates which served as the building block and mentioned earlier were investigated. These laminates were designated as 1F in the study since they were of one-laminate and had a fixed boundary condition during impact tests. The force–deflection curves of 18 1F specimens subjected to various levels of impact energy were shown in Fig. 3. The slope of the ascending section of each force–deflection curve was termed the *impact bending stiffness* due to its representation of the stiffness of composite laminates under impact-induced bending in the beginning of impact process. All the force–deflection curves seemed to ascend similarly, indicating similar impact bending stiffness. They then reached individual

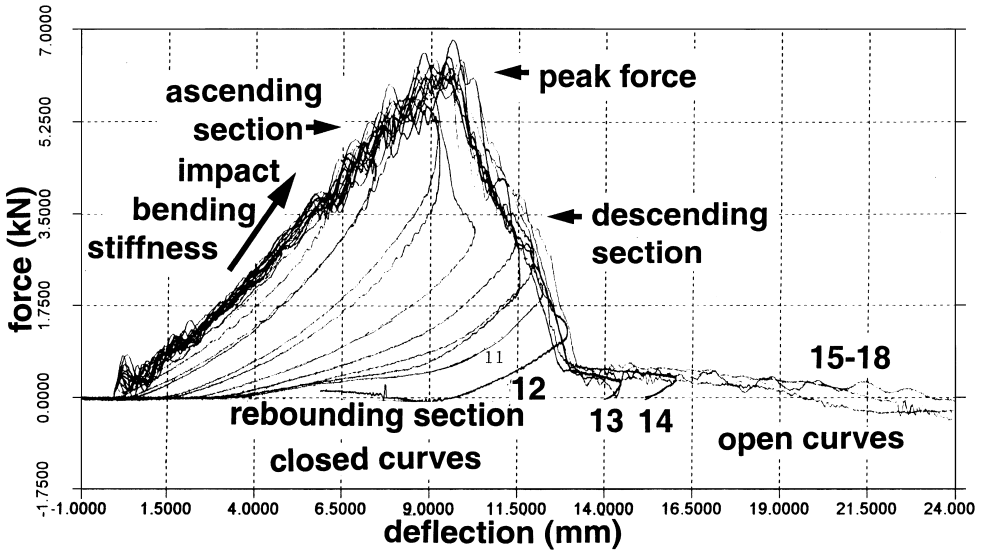

Fig. 3. Force–deflection curves of eighteen 1F composite plates.

maximum levels. According to Fig. 3, the maximum forces increased as the levels of impact energy increased. When the impact energy was high enough, the maximum forces seemed to have a similar value. This value was termed the *peak force* of the composite laminates under the specific central impact.

In each subperforation impact, the force–deflection curve rised, reached a maximum level and returned back to the origin. It formed a close curve representing the impactor's impacting onto the composite laminate and rebounding from the composite laminate. The area enveloped by the closed curve was the *absorbed energy* of the composite laminate under the specific impact. Apparently, as the impact energy increased, the enveloped area increased, so did the absorbed energy. If the impact energy continued to increase, perforation then took place. Once perforation occurred, the force–deflection curve would no longer be a closed curve. The area bounded by the open force–deflection curve and the deflection axis was then the energy absorbed by the perforated composite laminate. It was also interesting to point out that the impact events which had sufficiently high impact energy to reach the peak force seemed to share partial descending sections together. As a result, regardless of the rebounding sections, all the impact events seemed to form a master force–deflection curve.

3.2. Whole energy profile

As mentioned earlier, as far as residual properties were concerned, perforation seemed to cause the ultimate damage in composite laminates subjected to impact loading. Once a composite laminate was perforated, any excess impact energy would be retained as kinetic energy in the impactor except that an insignificant amount would be converted into additional damage. Hence, perforation threshold was an important parameter in characterizing the impact response of composite laminates [12–15]. Since peak force, contact duration and absorbed energy all reached critical levels when perforation took place [7], the perforation threshold of composite laminates could be identified through criteria based on the critical levels of peak force, contact duration, and absorbed energy. In addition, since impact energy should be completely absorbed by the composite laminates when perforation took place, the perforation threshold of composite laminates could be identified based on the equality between impact energy and absorbed energy [7].

Among the four criteria to identify the perforation threshold, the one based on equal energy between impacting and absorption was considered to be the most convenient and accurate technique [7]. Hence, a comparison between the impact energy and absorbed energy was required for judging the perforation threshold of composite plates. Results of eighteen 1F (one-laminate with fixed boundaries) specimens were given in Fig. 4. In addition to the experimental data points, a least-squares fitting curve for the data points with impact energy up to the penetration threshold and a least-squares line for the data points with impact energy beyond the perforation threshold were also identified. Shown in Fig. 4, the data points were represented by solid circles while the least-squares fittings by dashed lines. Apparently, as the impact energy increased, the absorbed energy also increased.

In addition to the raw data points and least-squares lines, a line representing the equality between impact energy and absorbed energy was also added to Fig. 4. It was called the *equal-energy line*. As could be seen from the diagram, the data points were quite lower than the equal-energy line when the impact energy was low. As the impact energy increased, the data points became closer to

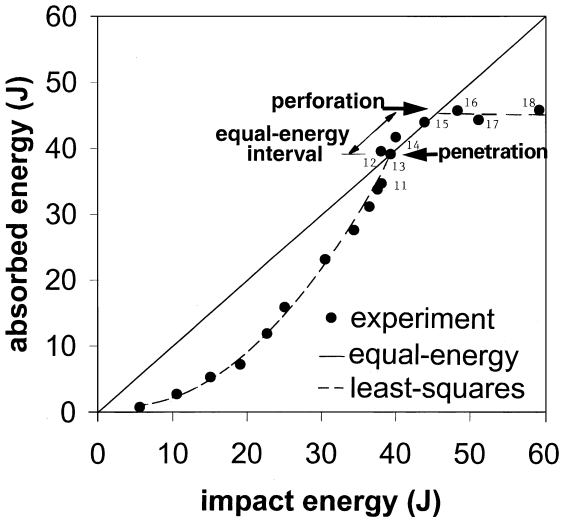

Fig. 4. The whole energy profile of 1F case based on force–deflection curves given in Fig. 3.

the equal-energy line. Eventually, the data points and the equal-energy line merged together. They then remained roughly the same for an interval until the data points became smaller than the equal-energy line again. The interval within that the data points overlapped with the equal-energy line was called the equal-energy interval. The discrepancy between the data points and the equal-energy line within the equal-energy interval as shown in Fig. 4 was believed to be caused by errors due to the numerical integrations mentioned earlier.

The equal-energy interval was bounded by two points. The point of lower bound was named *penetration threshold*, indicating the onset of penetration. When penetration took place, the impactor got stuck in the composite plate. Since very limited rebounding was allowed in the impactor, the impact energy was almost completely absorbed by the composite plate in forms of damage. As the penetration proceeded (the impactor moved deeper into the composite plate), it required more energy for the impactor to break through the composite plate and to overcome the friction between the impactor and the composite. Eventually, perforation of the composite plate would be achieved. Once perforation occurred, any excess impact energy would be retained in the impactor in form of kinetic energy, and the absorbed energy would be smaller than the impact energy again. Thus, there was an upper bound for the equal-energy line. The point of upper bound was called *perforation threshold*, indicating the completion of perforation process. Given in Fig. 4, the penetration threshold was about 38 J and the perforation threshold was around 45.5 J for the 1F case. The difference between the penetration threshold and the perforation threshold, i.e. the equal-energy interval, was believed to be dependent on the material type, the laminate thickness and the joining technique of the composite plate.

Fig. 4 was called the *whole energy profile* of the 1F (one-laminate with fixed boundaries) case since it included the overall energy exchange between the impactor and the composite plates. The diagram was derived directly from the force–deflection cuves given in Fig. 3. By closely comparing Fig. 3 with Fig. 4, it could be found that the force–deflection curves up to specimen no. 11 were of

Table 1
Impact bending stiffnesses, penetration thresholds and perforation thresholds of one- and two-laminate composite plates

Specimen type	Bending stiffness (N/mm)	Penetration threshold (J)	Perforation threshold (J)
1F: one-laminate fixed	933.0	38.0	45.5
2F: two-laminate fixed	1831.7	100.8	114.7
2T: double-sided taped	1740.4	104.7	111.1
2B: epoxy-bonded	3370.9	120.8	123.0
2R2: 2×2 riveting	1752.6	108.9	108.9
2R3: 3×3 riveting	1762.3	105.1	115.8
2R4: 4×4 riveting	1674.6	138.9	138.9
2RC: circular riveting	1694.5	105.9	123.8
2S3: 3×3 stitching	1670.0	103.5	115.0
2S5: 5×5 stitching	1663.0	108.2	120.0
2S9: 9×9 stitching	1559.1[a]	108.5[a]	108.5[a]
2BR3: bonded & riveted	3538.5	105.2	121.2
2BS3: bonded & stitched	2977.8	112.3	120.8

[a]Based on only one test.

closed type. Specimen nos. 12, 13 and 14 were located in the transition zone between closed curves and open curves. They were close to the penetration threshold. Once perforation took place, approximately around specimen no. 15, the curves changed from closed type to open type.

3.3. Penetration thresholds and perforation thresholds

The penetration and perforation thresholds of all assembled composite plates were identified from corresponding whole energy profiles and were given in Table 1. The 2R2 (2×2 riveting) case, however, had an identical value for both penetration threshold and perforation threshold because there was no intersection between its least-squares curve and the equal-energy line. A similar result also occurred in the 2R4 (4×4 riveting) case. These results were possibly due to experimental discrepancy. In addition, it should be pointed out that only one test was performed for 2S9 (9×9 stitching) case due to the very much time required for the specimen preparation.

Based on Table 1, the 2R4 (4×4 riveting) case had the highest perforation threshold and penetration threshold. By examining the damage of impacted plates, it was found that the four rivets closest to the center of each plate, i.e. closest to the impactor, were always seriously distorted by the impactor during the impact process. It was believed that the distortions of steel rivets resulted in additional energy absorption during impact. A special riveting pattern, namely 2RC (circular riveting), was then designed to avoid the problem and to verify the effects of high-density riveting on perforation threshold. The 2RC specimens had higher riveting density than the 2R4 specimens though the former was more locally concentrated and the latter globally distributed. The penetration threshold and the perforation threshold for the 2RC were 105.9 and 123.8 J, respectively, while they were both 138.9 J for the 2R4 case. Accordingly, the 2R4 case was not used for comparison in the remaining studies.

Among the two-laminate assembled composite plates, 2B (two-laminate bonded), 2RC (circular riveting), 2S5 (5×5 stitching), 2BR3 (bonded and 3×3 riveting) and 2BS3 (bonded and 3×3 stitching) had the perforation threshold close to 123 J while all others were between 108 and 115 J. It was believed that the adhesive bonding in the 2B, 2BR3 and 2BS3 cases contributed high rigidity and strength to the specimens, resulting in high-perforation thresholds. The high riveting density of 2RC and high stitching density of 2S5 also made similar contribution to individual specimens. In fact, the perforation threshold increased as the riveting density increased from 2R2 (2×2 riveting) to 2R3 (3×3 riveting), and to 2RC. Similarly, the perforation threshold increased as the stitching density increased from 2S3 (3×3 stitching) to 2S5. Due to the single test for the 2S9 (9×9 stitching) case, the result was inconclusive and omitted from further discussion.

Although high density of riveting and stitching seemed to make positive contribution to perforation threshold, it should be noted that their preparations also required extra effort in both time and labor task. Besides, it was also possible that they introduced extra damage, i.e. holes, to the assembled composite plates. By examining the penetration thresholds of 2B (two-laminate bonded), 2BR3 (bonded and 3×3 riveting) and 2BS3 (bonding and 3×3 stitching) cases, the 2B case with penetration threshold of 120.8 J outperformed the remaining two cases which had 105.2 and 112.3 J, respectively. Accordingly, the experimental results seemed to indicate that pure epoxy bonding was sufficiently efficient for joining thin composite laminates. The additional riveting and stitching might cause more damage to composite laminates than effectively join them. The penetration thresholds of all other cases were between 100.8 and 108.9 J and were much lower than the 2B case. This result further confirmed the superiority of the joining efficiency of epoxy bonding in assembling thin (3.2 mm) composite laminates. In addition, it should be noted that the equal-energy intervals for all two-laminate composite plates seemed to be very similar.

3.4. Impact bending stiffness

Bending stiffness had been found to be an important parameter to delamination resistance [16] and perforation resistance [7]. In investigating the effects of joining technique on perforation resistance, the bending stiffnesses, which were the slopes of the force–deflection curves, of various assembled composite plates were identified and also listed in Table 1. Results of the two-laminate plates could be essentially divided into two groups. The bending stiffnesses of 2B (two-laminate bonded), 2BR3 (bonded and 3×3 riveting) and 2BS3 (bonded and 3×3 stitching) cases were from 3000 to 3500 N/mm. These values were about two times those of the remaining two-laminate cases. Since the impact bending stiffness changed with the type of assembled composite plates, it in fact was associated with the joining stiffness due to the corresponding joining technique. Hence, the impact bending stiffness could be considered as an index of joining stiffness up to some extent.

The perforation thresholds and bending stiffnesses of two-laminate plates were put together in Fig. 5. Apparently, there was a correlation between them. That was, higher the bending stiffness of an assembled composite plate, higher the penetration and perforation thresholds. However, when compared with those of the one-laminate case, i.e. 1F, the increase in penetration and perforation thresholds seemed to be more significant due to thickness increase than due to bending stiffness increase. In fact, by adding one more laminate to the one-laminate plates to become two-laminate plates, both energy thresholds and bending stiffness were almost doubled. However, an increase in

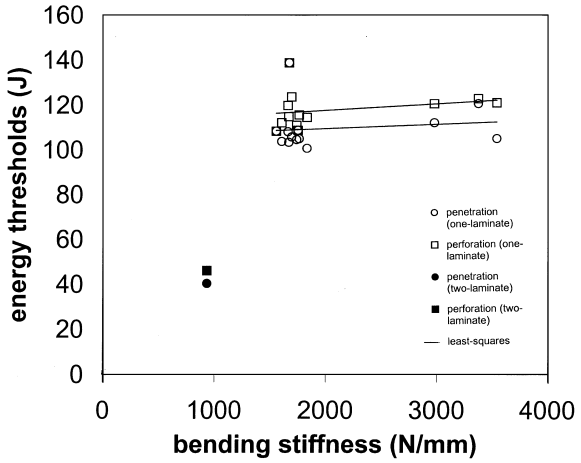

Fig. 5. Relation between energy thresholds and impact bending stiffness of various two-laminate composite plates.

bending stiffness based on any joining technique did not seem to improve the penetration and perforation thresholds significantly.

3.5. Laminated plates versus assembled plates

In verifying the feasibility of using assembled composite plates to replace laminated composite plates, a study comparing the impact bending stiffnesses and perforation thresholds of these two groups was necessary. In this study, besides the 1F (3.2 mm thick) case, two other types of composite laminate were investigated. These two types of composite laminate had cross-ply laminations and thicknesses of 2.24 and 6.66 mm. They were designated as 1F-2.24 and 1F-6.66. Their whole energy profiles were given in Fig. 6 along with the 1F-3.2 case. Apparently, all of them had similar trends, and the equal-energy interval increased from 5 J for 1F-2.24 to 7.5 J for 1F-3.2, and to 40 J for 1F-6.66. This result confirmed that the equal-energy interval, or the penetration process, was dependent on the thickness of composite plates.

In order to further confirm that thickness, instead of bending stiffness, played a more efficient role in improving perforation resistance, an investigation on thickness effects was performed. The composite laminates used in this study were of 1F-2.24. They had material properties identical to those of 1F-3.2 specimens. However, their stacking sequence was $[0/90/0/\ldots]_9$ and nominal thickness was 2.24 mm. In addition to the 1F-2.24 case, assembled composite plates such as 2F-2.24 (two-laminate with fixed boundaries), 2B-2.24 (two-laminate bonded) and 4F-2.24 (four-laminate with fixed boundaries) cases were created. Their whole energy profiles were presented in Fig. 7 for comparison. Although the difference of impact bending stiffnesses between 2F-2.24 and 2B-2.24 was as much as that between 2F and 2B (both based on 3.2-mm laminates) cases, their whole energy profiles were very similar. However, the whole energy profiles of 1F-2.24, 2F-2.24 and 4F-2.24 were quite different. Apparently, the thicker the assembled composite plate, the higher the capability of energy absorption. According to Fig. 7, the penetration thresholds for 1F-2.24, 2F-2.24, 2B-2.24

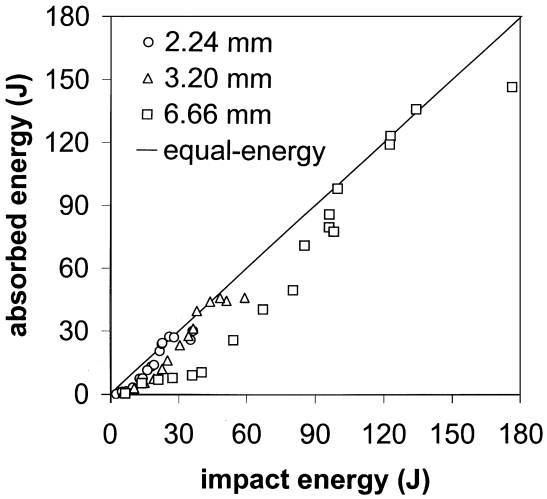

Fig. 6. The whole energy profiles of three-laminated composite plates.

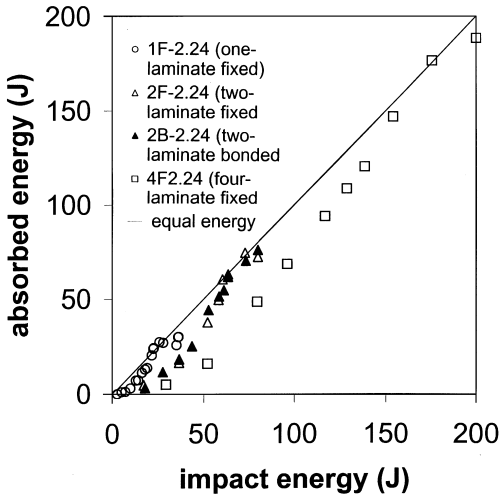

Fig. 7. The whole energy profiles of four assembled composite plates.

and 4F-2.24 were about 22, 63, 62 and 157 J, respectively, and the perforation thresholds for them were about 27, 73, 73 and 182 J, respectively. The equal-energy intervals, i.e. the difference between the penetration thresholds and the perforation thresholds, for the four cases were thus 5, 10, 11 and 25 J. This result combined with those of earlier studies provided evidence that the equal-energy interval was dependent on the thickness of composite plates.

The perforation thresholds of both assembled cases, including 1F-2.24, 2F-2.24, 2B-2.24, 2F-3.2, 2B-3.2, 4F-2.24, and laminated cases, including 1F-2.24, 1F-3.2 and 1F-6.66, were also summarized

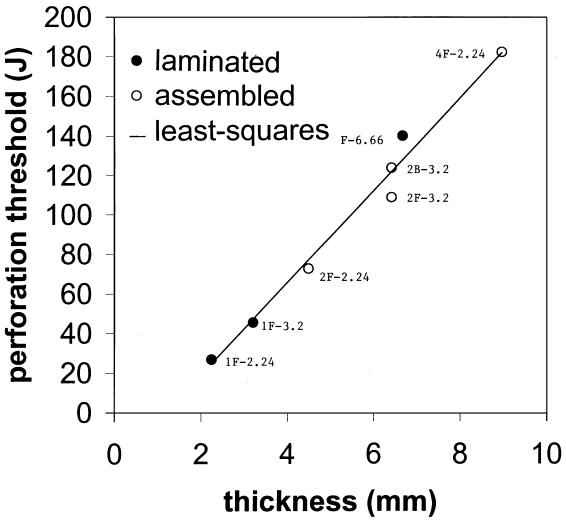

Fig. 8. The relation between perforation threshold and thickness for both laminated and assembled composite plates.

in Fig. 8 for comparison. Apparently, the assembled cases were very similar to the laminated cases because they were all closely located along a least-squares line. It then could be concluded that the perforation threshold of a composite plate was dependent on thickness only, regardless of being laminated or assembled. In other words, the assembled composite plates could be used as alternatives for thick laminated composite plates, at least, as far as the perforation threshold was concerned.

4. Conclusions

The following conclusions can be drawn from the above investigations:

(1) Various joining techniques such as mechanical riveting, adhesive bonding, joining and their combinations were used in assembling two- and four-laminate composite plates. Pure epoxy bonding was found to be the most efficient joining technique in assembling the composite laminates together since it gave the highest bending stiffness and perforation threshold.

(2) Among the assembled two-laminate composite plates, the perforation threshold increased as the bending stiffness increased. However, the increase of perforation threshold based on the improvement of bending (joining) stiffness was limited. A more efficient way to significantly increase the perforation threshold was to increase the thickness of composite laminates, or to use assembled multi-laminate composite plates.

(3) A technique named whole energy profile was presented for characterizing impact-perforation resistance. When penetration took place, the absorbed energy was approximately equal to the impact energy. When perforation occurred, the absorbed energy was again smaller than the impact energy. Experimental results revealed that the equal-energy interval, which was the difference

between the penetration threshold and perforation threshold, increased as the thickness of composite plates increased.

(4) Based on these studies, it was found that assembled composite plates were comparable with laminated composite plates in both bending stiffness and perforation threshold. This result verified the advantage of using assembled composite plates over thick laminated composite plates since the cost of making thick laminated composite plates with high quality increased significantly as the thickness increased.

Acknowledgements

This investigation was supported by both Michigan Research Excellence Fund and the U.S. Army TACOM-TARDEC ILIR program. The authors wish to express their sincere thanks for the financial supports.

References

[1] Workshop on Scaling Effects in Composite Materials and Structures, NASA Langley Research Center, Hampton, VA, Report No. 94-6, Institute for Mechanics and Materials, University of California, San Diego, California, November 15–16, 1993.
[2] Carpinteri A, Editor. Size-scale effects in the failure mechanisms of materials and structures. E & FN Spon, 1994.
[3] Rajapakse YDS, Editor. Mechanics of Thick Composites. The American Society of Mechanical Engineers 1993: AMD-Vol. 162.
[4] Morton J. Scaling of impact-loaded carbon-fiber composites. AIAA J 1988;26(8):989–94.
[5] Qian Y, Swanson SR, Nuismer RJ, Bucinell RB. An experimental study of scaling rules for impact damage in fiber composites. J Compos Mater 1990;24(5):559–70.
[6] Sankar BV. Scaling of low-velocity impact for symmetric composite laminates. J Reinforced Plast Compos 1992;11:297–305.
[7] Liu D, Raju BB, Dang X. Size effects on impact response of composite laminates. Int J Impact Engng 1998;21(10):837–54.
[8] Wei J, Hawley MC, DeLong J, DeMeuse M. Comparison of microwave and thermal cure of epoxy resins. Polym Engng Sci 1993;33(17):1132–40.
[9] Lee C, Liu D. Tensile strength of stitching joint in woven glass fabrics. J Engng Mater and Technol 1990; 112(2):125–30.
[10] Liu D. Photoelastic study on composite stitching. Exp Tech 1990;14(1):25–7.
[11] Liu D. Delamination resistance in stitched and unstitched composite plates subjected to impact loading. Reinforced Plast Compos 1990;9(1):59–69.
[12] Wu E, Tsai E-Z, Chen Y-C. Penetration into glass epoxy composite laminates. J Compos Mater 1994;28:1783–802.
[13] Sun CT, Potti SV. High velocity impact and penetration of composite laminates. Proceedings of the Ninth International Conference on Composite Materials 1993; Vol. 4. p. 157–165.
[14] Goldsmith W, Dharan CKH, Chang H. Quasi-static and ballistic perforation of carbon fiber laminates. Int J Solid Struct 1995;32:89–103.
[15] Lee SWR, Sun CT. Dynamic penetration of graphite/epoxy laminates impacted by a blunt-ended projectile. Compos Sci Technol 1993;49:369–80.
[16] Liu D. Impact-induced delamination — a view of material property mismatching. J Compos Mater 1988;22(7): 674–91.